

# Motion prediction and delay compensation for improved teleoperation of an exoskeletal robot

Pu Duan<sup>1</sup>, Zhuoping Duan<sup>1</sup>, Shilei Li<sup>2</sup> and Yawen Chen<sup>3</sup>

## Abstract

Delay is a major challenge in teleoperation. To teleoperate a robot in real-time with specific human motion such as walking, prediction and compensation algorithms are needed to minimize the tracking delay. Human walking possesses the inherent features of synergy and quasi-periodicity with nonlinearity. By analyzing these features, three prediction methods were designed. A delay-coordinate phase space reconstruction method is based on the delay embedding theorem and uses the historical data. The echo prediction method uses data from the coupling joints of the other body side and takes the Euclidean distances in the delay-coordinate phase space reconstruction method for data search and match. The fused prediction method combines the delay-coordinate phase space reconstruction and echo prediction methods, uses the best matching historical data of the same joint and the corresponding joint of the other limb. These methods were implemented for teleoperation of an exoskeletal robot with inertial measurement unit measurements of human walking. The predicted trajectories were used to compensate the teleoperation delay and improve the robot tracking performance. Experimental results demonstrated that the fused method brought apparent improvement over other methods and can serve as a promising solution for time delay estimation, prediction, and compensation of human walking tracking and teleoperation.

## Keywords

Robot teleoperation, motion prediction, delay compensation, delay-coordinate phase space reconstruction, echo control, data fusion

Date received: 9 July 2017; accepted: 26 January 2018

Handling Editor: Fei Chen

## Introduction

Teleoperation of exoskeletal robots is an essential approach for rehabilitation and many other applications. For patients that suffer from neurological injuries and resulted functional disabilities, they need help on body limbs movements and trainings. Complex tasks such as human walking require multi-joint coordination, are functionally difficult and physically challenging for both the therapists and patients. Furthermore, the limited number of experienced therapists and increased rehabilitation training need necessitate remote rehabilitation. These strong needs motivate the teleoperation of lower limb exoskeletal robots.<sup>1–5</sup>

Mechanical motion capture systems are often used in early days<sup>6,7</sup> and brain machine interface is emerging.<sup>8</sup> The motion capture systems composed of inertial

<sup>1</sup>State Key Laboratory of Explosion Science and Technology, Beijing Institute of Technology, Beijing, China

<sup>2</sup>School of Mechanical Engineering and Automation, Harbin Institute of Technology Shenzhen Graduate School, Shenzhen, China

<sup>3</sup>Xeno Dynamics Co., Ltd, Shenzhen, China

## Corresponding author:

Zhuoping Duan, State Key Laboratory of Explosion Science and Technology, Beijing Institute of Technology, No. 5, Zhongguancun South Street, Haidian District, Beijing 100081, China.

Email: duanzp@bit.edu.cn



measurement units (IMUs) have many attractive advantages. They are technically sound, reliable, economically efficient, informative, can be made compact and light weight. Furthermore, they are wearable and do not obstruct human movements. Although the accuracy is often lower than mechanical systems, it is sufficient for human motion capture such as walking tracking. Therefore, IMU-based motion capture systems have come to be a feasible and popular solution.<sup>9–13</sup>

Tracking strategies such as force tracking and trajectory tracking have been widely used.<sup>14</sup> Trajectory tracking is inherently more stable and robust and has been widely used for various industrial applications. The force tracking by itself bears some complications and limitations.<sup>7</sup> One main challenge for force tracking is that a precise dynamic model of the operator is needed to obtain the required force. However, it is inevitable that delay happens when the kinematic data of the operator captured by IMUs are obtained, processed, transferred to the robot to be implemented. Delay compensation for joints' motion is intuitively exploited with different prediction methods.

Human walking is a quasi-periodic process exhibiting certain chaos features,<sup>15</sup> which indicates the nonlinear characteristics of human musculoskeletal dynamic systems. During walking, the two lower limbs operate with synergy.<sup>16,17</sup> These features inspire motion estimation, prediction, and compensation methods of this research.

Based on the synergy feature of human walking, echo control has been proposed and applied in powered prosthesis by many researchers.<sup>18,19</sup> This method generates joint's trajectories of one limb by a phase shift of the other limb during human walking.<sup>20</sup> However, problem exists in how to determine the time shift. As an improvement of echo control, the complementary limb motion estimation (CLME) method<sup>21</sup> assumes a coupling relationship between two lower limbs. The regression method has significant influence on performance and should be carefully determined.<sup>22</sup> Based on the quasi-periodic nonlinear dynamic feature of human locomotion, the delay-coordinate phase space reconstruction (DPSR) method originating from Takens' Reconstruction Theorem is a widely used method for nonlinear time series dynamic factor analysis. This can be used to predict the trajectories,<sup>23,24</sup> but such method requires historical data prior to a reasonable performance. There are also other prediction and compensation methods, such as the autoregressive integrated model method, autoregressive integrated moving average method, autoregressive moving average model method,<sup>3</sup> modified recursive least square method,<sup>4</sup> neural network-based method.<sup>25,26</sup>

Here, in this work, a novel method for prediction and compensation of human walking has been

proposed based on the fusion of the echo prediction and DPSR prediction methods and then implemented for teleoperation of a lower limb exoskeleton robot. Experiments have been conducted to examine the feasibility and efficacy of the proposed method and to compare with the echo control and DPSR methods.

The paper is organized as follows. Section “The teleoperation system” introduces the exoskeletal robot teleoperation system. Section “Delay prediction and compensation methods” describes the echo control method, DPSR method, and our fused method. Section “Experiments and results” shows the implementation, experiments, and results. Finally, section “Conclusion” concludes this work.

## The teleoperation system

The teleoperation paradigm from human walking to the exoskeletal robot is illustrated in Figure 1. The developed motion capture system based on IMUs is shown in Figure 2. The attaching structures are designed to fit the shape of human lower limbs with Velcro straps. The execution robot is the PXMZ1 lower extremity exoskeletal robot developed by Xeno Dynamics Co., Ltd., which consists in total of 10 DoFs. Four actuated joints (extension/flexion of knees and hips) are included in its sagittal plane and six passive joints (adduction/abduction and rotation of hips and flexion/extension of ankles) are fixed during experiments. The robot is fixed on a test jig via its wrist, as shown in Figure 3. The human operator walks on a treadmill equipped with the motion capture system. During operation, the hip and knee joints' motion of the robot tracks that of the human in sagittal plane with data collected by the IMU-based motion capture system. The robot joints' motion data could be collected with its own encoders simultaneously.

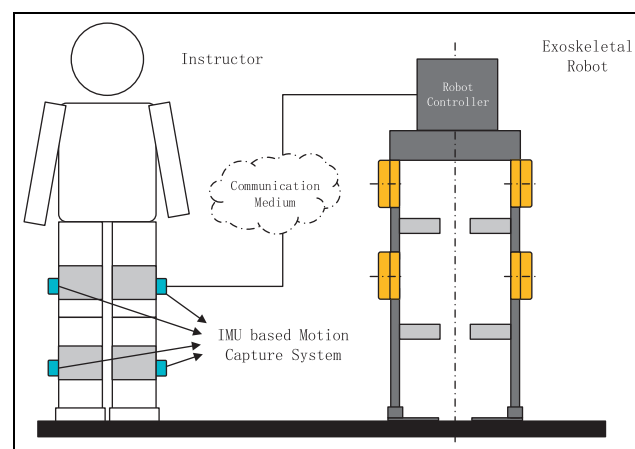


**Figure 1.** The teleoperation paradigm from human walking to the exoskeletal robot.

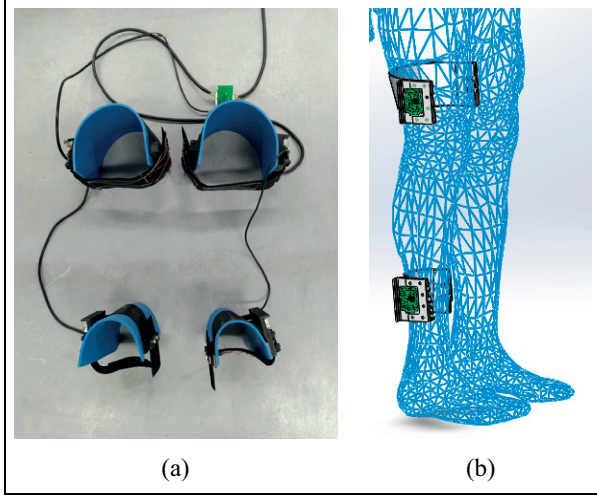


**Figure 2.** The IMU-based lower limb motion capture system: (a) IMU-based measurement hardware and (b) illustration of attachment to human.

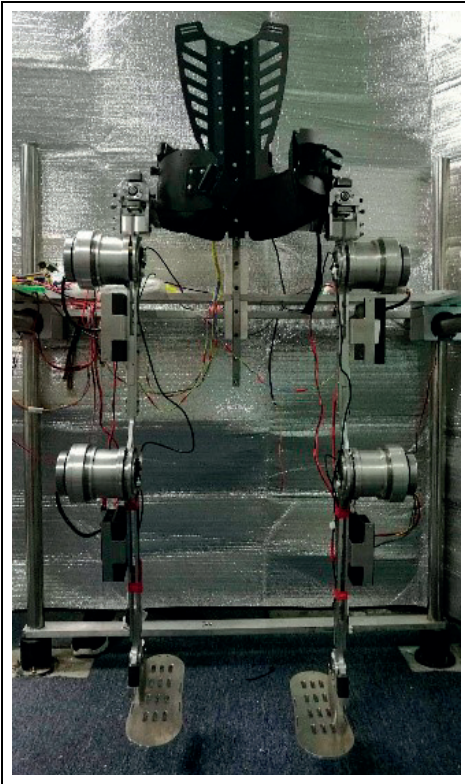


**Figure 3.** The PXMZI lower extremity exoskeletal robot in experimental configuration.

## Delay prediction and compensation methods

### The DPSR prediction method

Human locomotion has the inherent quasi-periodic and nonlinear dynamic feature, and the DPSR method can

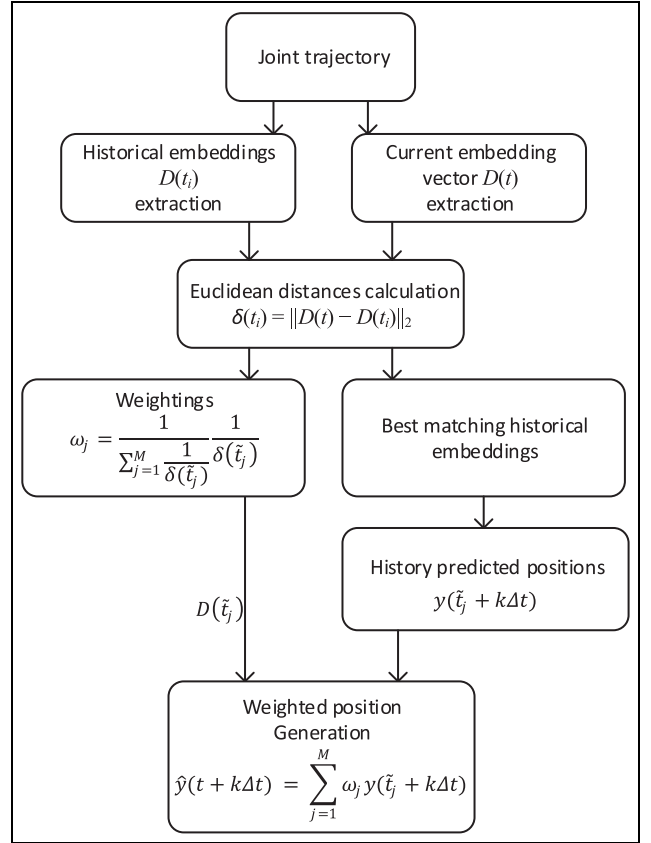


**Figure 4.** The DPSR prediction workflow.

be adopted to predict the joints' trajectories of the human lower limbs. According to Takens' Reconstruction Theorem, it is possible to reconstruct the dynamics of a nonlinear system based on its previous measurements. A current embedding vector, also called reconstruction vector, is extracted by incorporating  $p$  past observations with a time delay of  $h$  sampling instants between subsequent components

$$D(t) = [y(t) \quad y(t-h) \quad \cdots \quad y(t-h(p-1))]^T \quad (1)$$

where  $t$  is the current sampling time point. The algorithm proposed by Herrmann<sup>24</sup> is illustrated in Figure 4.

At each sampling time point  $t$ , an current embedding vector  $D(t)$  is acquired. For accomplishing predictions, the current embedding vector  $D(t)$  is compared to all collected historical embeddings  $D(t_i)$  with  $t_i < t$  by determining the Euclidean distances  $\delta(i) = \|D(t) - D(t_i)\|_2$ . The  $M$  best matching embeddings  $D(\tilde{t}_1), D(\tilde{t}_2), \dots, D(\tilde{t}_M)$  from the sampling instants  $\tilde{t}_j$  with  $1 \leq j \leq M$  are used to calculate a  $k$ -step prediction  $\hat{y}(t + k\Delta t|t)$

$$\hat{y}(t + k\Delta t|t) = \sum_{j=1}^M \omega_j y(\tilde{t}_j + k\Delta t) \quad (2)$$

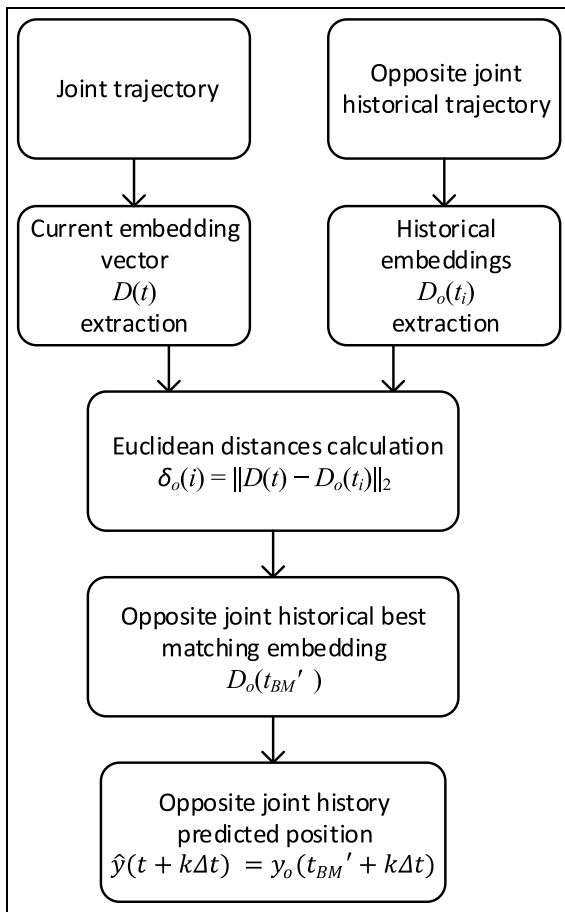


**Figure 5.** The echo prediction workflow.

with the weightings

$$\omega_j = \frac{1}{N} \frac{1}{\delta(\tilde{t}_j)} \quad (3)$$

and

$$N = \sum_{j=1}^M \frac{1}{\delta(\tilde{t}_j)} \quad (4)$$

### The echo prediction method

Inspired by the mathematical idea that the Euclidean distances can be used in the DPSR method to search and match the data, the echo prediction method based on the coupling relationship between the left and right lower limbs has been proposed, as shown in Figure 5. The current embedding vector  $D(t)$  of one joint trajectory is compared to the collected historical embeddings  $D_o(t_i)$  with  $t_i < t$  by determining the Euclidean distances  $\delta(i) = \|D(t) - D_o(t_i)\|_2$ , but the difference is that the collected embeddings  $D_o(i)$  are generated by the joint of the opposite lower limb. The position  $y_o(t_n + k\Delta t)$  that

$k$  steps after the best matching vector  $D_o(t_{BM}')$  is the position to be predicted on the trajectory.

Here only one best matching embedding  $D_o(t_{BM}')$  is used. This is because M only introduces an additional degree of freedom to be less prone to noisy data by averaging the effects of noise from different samples,<sup>24</sup> while the human historical motion data are not noisy. The jumps in predicted result are mainly generated by amplitude offsets between the past observation and the current position and lack of similar historical data. Offset correction is an important part of the fused method. Also, larger  $M$  is directly related to computational cost, which is also a factor needed balancing in real-time execution. The fused prediction methods also used only one best matching vector.

### The fused prediction method

The fused method combines the best matching historical trajectory data of the same joint and the corresponding joint of the other side lower limb. It is expected that the fused trajectories predicted would be more accurate, and the method would be faster to converge and more stable during the unstable conditions than the previous elaborated methods. The fused prediction method is described in Figure 6.

As previously described in the last two methods if the best matching embeddings  $D(t_{BM}), D_o(t_{BM}')$  for two corresponding joints of each limb are found (one best embedding for each joint), they are corrected by a shift forming  $D_s(t_{BM}), D_{os}(t_{BM}')$ , which is the difference between the last position of the best matching embeddings and the current embedding, in order to eliminate the jumps of the predicted positions over the current positions. The predicted position  $k$  steps ahead,  $\hat{y}(t + k\Delta t|t)$ , is simply fused with two weightings  $\omega_E$  and  $\omega_{oE}$  as

$$\hat{y}(t + k\Delta t|t) = \omega_E y_s(t_{BM} + k\Delta t) + \omega_{oE} y_{os}(t_{BM}' + k\Delta t) \quad (5)$$

The question evolves into how to decide the two weightings in a dynamic and reasonable manner. It is not reasonable to decide the weightings based on the predicted positions only, so the current embedding vector forms two vectors,  $Ex(t_{BM})^{appending}$  and  $Ex_o(t_{BM}')^{appending}$ , by appending the two predicted  $k$ -step vectors  $P(t_{BM})$  and  $P_o(t_{BM}')$  separately. The obtained extended vectors represent the trajectories combining the past and possible future. Similarly, the two best matching embeddings are extended to  $p + k$  steps vectors,  $Ex(t_{BM})$  and  $Ex_o(t_{BM}')$ , representing the corresponding past observations. Figure 7 shows the process in details.

The correlation values,  $\alpha_{a-E}$  and  $\alpha_{a-oE}$ , between the possible trajectories  $Ex(t)^{appending}$  and its corresponding

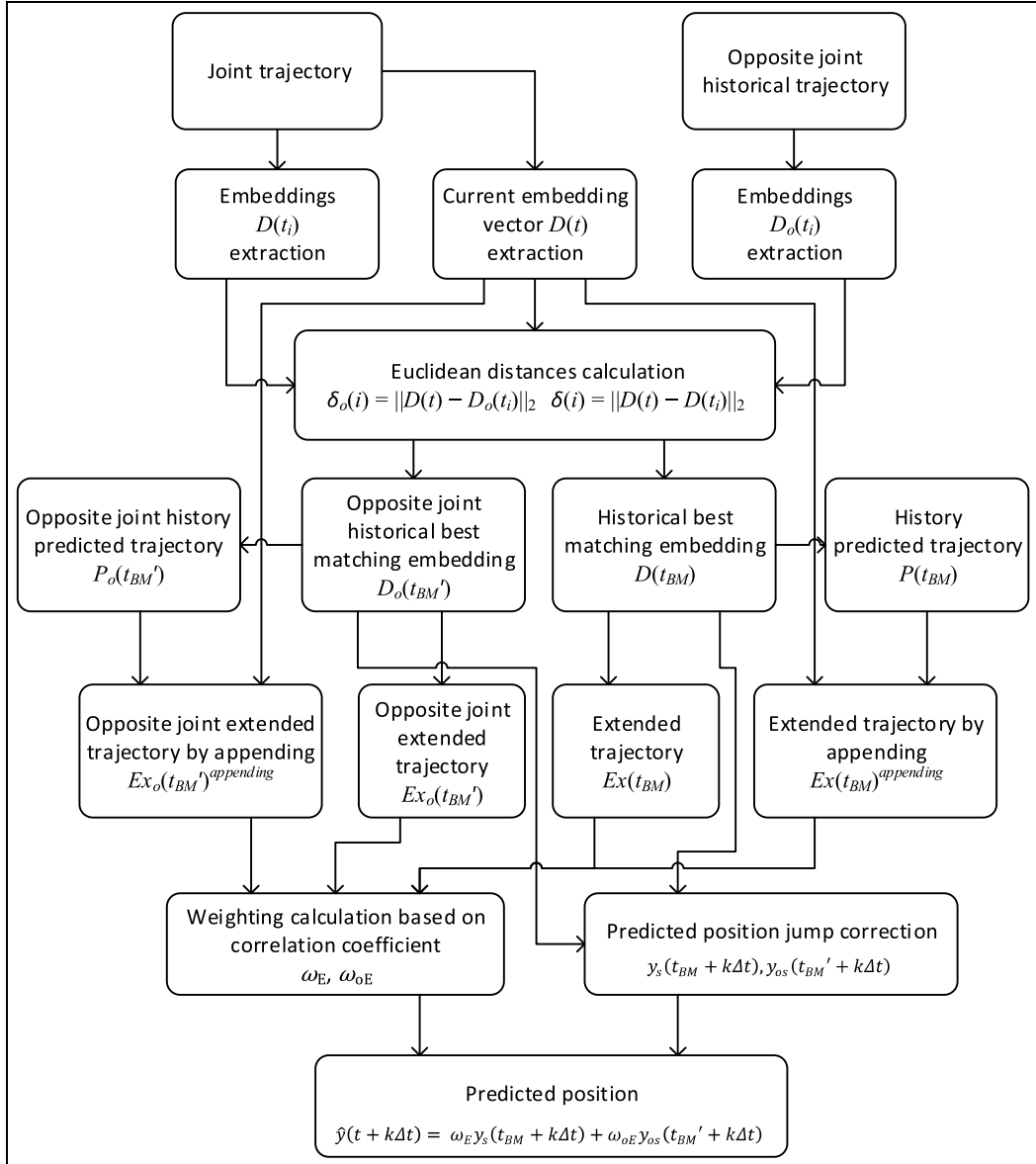


**Figure 6.** The proposed algorithm based on the fusion of DPSR and echo prediction.

historical observations  $Ex(t_{BM})$  and  $Ex_o(t_{BM}')$  are computed. They stand for the similarity between the possible future trajectory and its past observations.  $\alpha_{oa-E}$  and  $\alpha_{oa-oE}$  are obtained in the same way. We hope the two possible trajectories not only have high similarity with their two past observations, but also deviate not too much from both of the past observations from the left and right limbs. The expectations and deviations of  $\alpha_{a-E}$ ,  $\alpha_{a-oE}$  and  $\alpha_{oa-E}$ ,  $\alpha_{oa-oE}$  are  $E_a$ ,  $D_a$  and  $E_o$ ,  $D_o$ . High expectations are preferred, while high deviations are undesired. Bringing them together and the normalized weightings are

$$\omega_E = \frac{1 - E_o + D_o}{(1 - E_a + D_a) + (1 - E_o + D_o)} \quad (6)$$

and

$$\omega_{oE} = 1 - \omega_E \quad (7)$$

respectively. And the  $k$ -step prediction is determined by equation (5).

#### Delay compensation

The estimated delay time  $k\Delta t$  is obtained by the difference between the last time point of the embedding vector  $D_r(t)$  of the robot and the best matching embedding of the operator. As the delay time  $k\Delta t$  exists, the predicted human joint angle position  $\hat{y}(t + k\Delta t)$  at the time of  $k\Delta t$  ahead is sent to the actuator to achieve

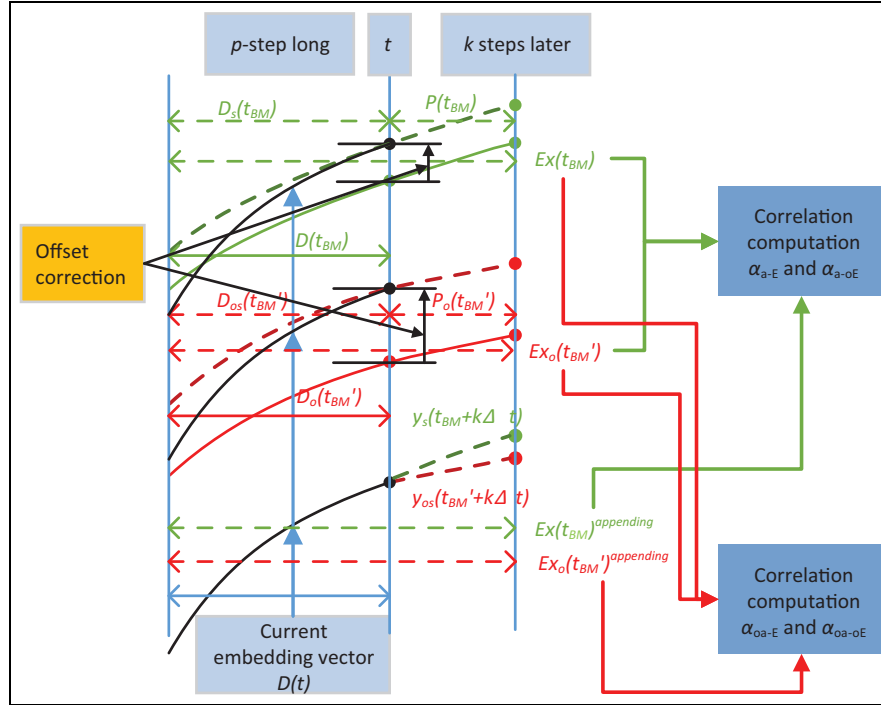


**Figure 7.** The construction of extended vectors and their correlation calculation.

compensation in each controlling cycle as demonstrated in Figure 8. The actual output of the corresponding robot joint angle position  $y_r(t)$  is the compensated result. The delay estimation and compensation methods were the same for all methods in this research.

## Experiments and results

### Experimental design

Four experiments were carried out, one as baseline and three with different prediction compensation methods implemented. During the experiments, the exoskeletal robot was fixed on a stationary frame with its operator walking parallel on a treadmill. The actual experimental scenario could be seen in Figure 9(a). The acquisition frequency and control frequency were both 50 Hz. Each time a dataset of the left hip, right hip, left knee, and right knee joints' angle in sagittal plane of the robot and test subject with a length of 90–100 s was collected simultaneously. The human motion data were collected by the IMU-based motion capture system. The robot motion data were collected with its encoders. The hip and knee joints' angles used in this research are defined as seen in Figure 9(b). Before the experiments, static calibration was done to ensure the IMU measured

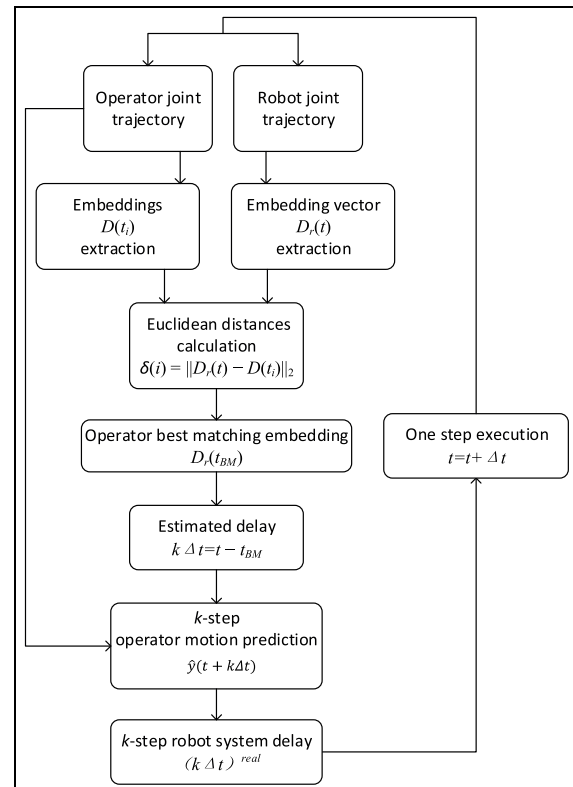


**Figure 8.** Delay time estimation and compensation.

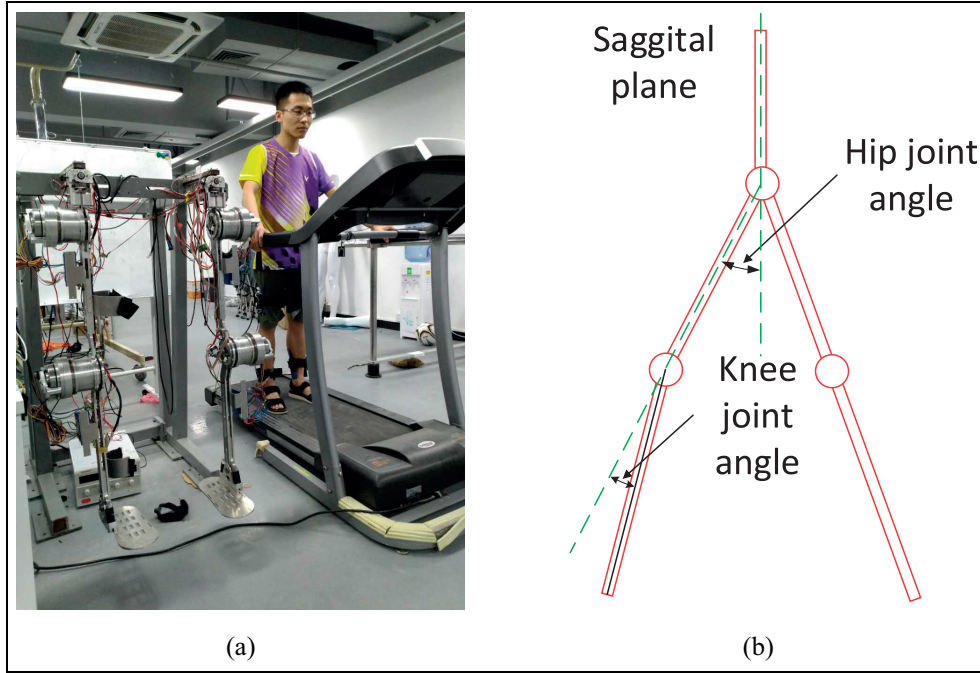


**Figure 9.** Experimental configurations: (a) experimental scenario and (b) human hip and knee joint's angles collected during experiments by the IMU-based motion capture system.

human joint angles and the robot encoder measured joints' angles in the sagittal plane were the same.

The data collection included five typical walking segments: walking initiation, stable walking at 0.8 km/h, speed transition from 0.8 to 1.4 km/h, stable walking at 1.4 km/h, and walking termination. The performance during initiation, transition, and termination decides whether the prediction methods are applicable to real human walking and this is one key evaluation criterion of algorithm excellence. Specially, the baseline data with five segmentations were demonstrated in Figure 10.

### Assessment measures

To quantify the algorithms' compensation performance, the prediction ratio (PR), tracking ratio (TR), and overall compensation ratio (OCR) were selected as metrics.<sup>24</sup> PR represents the prediction errors between the predicted human joints' trajectory  $\hat{y}(t|t - k\Delta t)$  and real human joints' trajectory  $y(t)$  calculated by

$$PR(y(t), e(t)) = 1 - \frac{RMS(e_{PR}(t))}{RMS(y(t))} \times 100\% \quad (8)$$

where

$$e_{PR}(t) = \hat{y}(t|t - k\Delta t) - y(t) \quad (9)$$

TR represents the tracking errors between the predicted human joints' trajectory  $\hat{y}(t|t - k\Delta t)$  and the compensated robot joints' trajectory  $y_r(t)$  calculated by

$$TR(y(t), e(t)) = 1 - \frac{RMS(e_{TR}(t))}{RMS(y(t))} \times 100\% \quad (10)$$

where

$$e_{TR}(t) = y_r(t) - \hat{y}(t|t - k\Delta t) \quad (11)$$

OCR represents the overall errors between the predicted human joints' trajectory  $y(t)$  and the robot joints' trajectory  $y_r(t)$  calculated by

$$OCR(y(t), e(t)) = 1 - \frac{RMS(e_{OCR}(t))}{RMS(y(t))} \times 100\% \quad (12)$$

where

$$e_{OCR}(t) = y_r(t) - y(t) \quad (13)$$

### Baseline results

The experiment without compensation was conducted as the baseline, which presented a delay of 40–60 ms approximately at the speed of 0.8–1.4 m/s (see Figure 11(a)). Such delay mainly came from the communication and response frequency of the motor controllers, the motors' driving ability, and the actuation modules' dynamic characteristics. The delay of the whole process was unidirectional and the highlighted segments of the knee joints' trajectories in Figure 11(a) exhibited much longer delay. The reason was that the execution delay always existed and the robots' knee joints could hardly meet the performance requirement during the

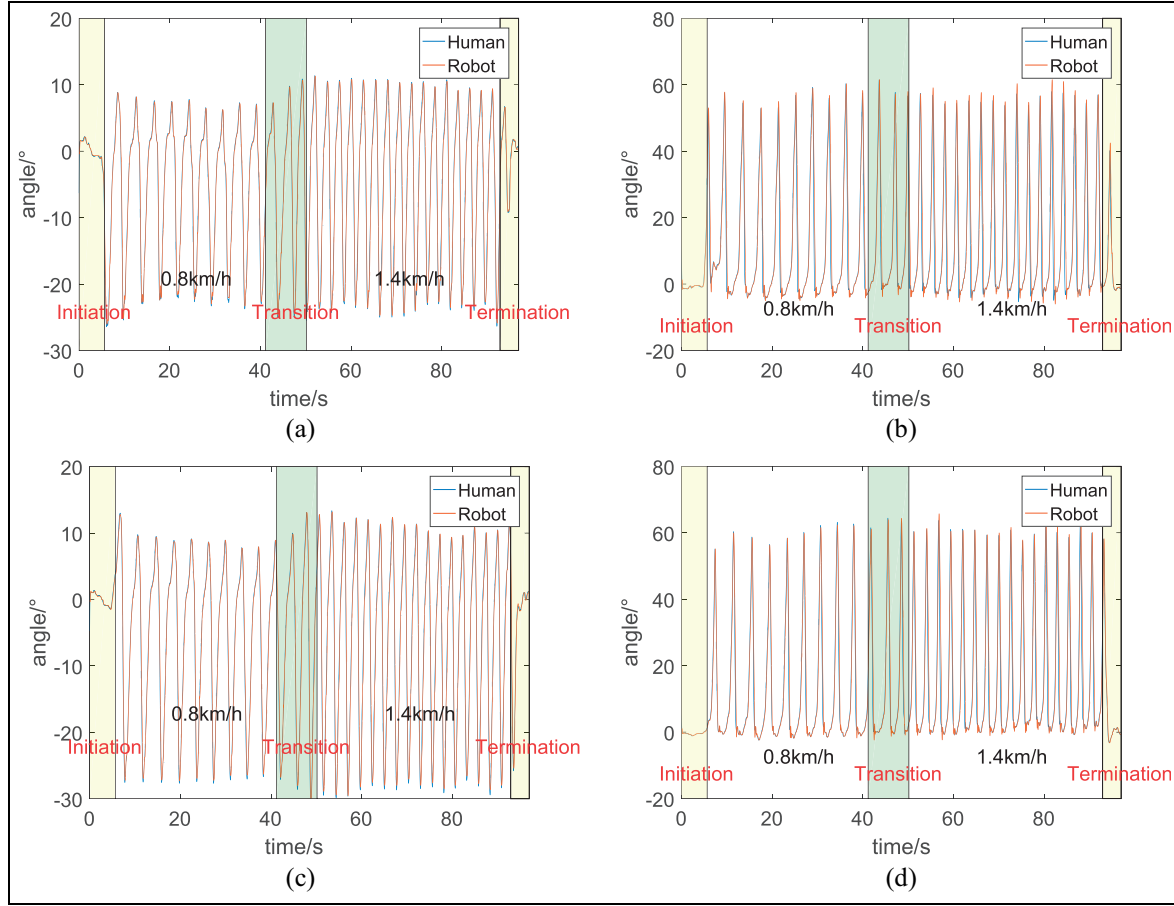


**Figure 10.** Baseline joints' trajectories without compensation marked as five segments: (a) left hip, (b) left knee, (c) right hip, and (d) right knee.

**Table I.** Performance of different methods comparing with the baseline.

	Left hip			Left knee			Right hip			Right knee		
	PR	TR	OCR	PR	TR	OCR	PR	TR	OCR	PR	TR	OCR
Baseline	0.909	0.961	0.883	0.826	0.786	0.662	0.910	0.960	0.879	0.839	0.867	0.748
Echo	0.762	0.899	0.751	0.818	0.705	0.628	0.860	0.913	0.837	0.864	0.842	0.846
DPSR	0.869	0.895	0.842	0.870	0.746	0.727	0.885	0.907	0.855	0.904	0.871	0.842
Fused	0.964	0.943	0.933	0.957	0.831	0.823	0.966	0.944	0.933	0.962	0.917	0.911

PR: prediction ratio; TR: tracking ratio; OCR: overall compensation ratio; DPSR: delay-coordinate phase space reconstruction.

highlighted time. Thus, PR and TR were needed to quantify the performance of prediction and execution separately during the compensation process.

For the baseline experiment, the collected human joints' motion data were sent directly to the exoskeletal robot for execution. As the human trajectories were  $y(t)$ , the predicted trajectories could be taken as  $\hat{y}(t) = y(t - k\Delta t|t)$  which meant the assumed prediction method imposed a delay what was prediction in the other methods. And the PRs, TRs, and OCRs could be computed normally as listed in Table 1.

### Results with motion prediction and delay compensation

During the implementation of all the proposed methods, the maximum number of steps to be predicted was set to be three. This meant they were capable of compensating a delay of less than 60 ms, as the sampling interval of the motion capture system was 20 ms. The embedding vectors had a length of 30 steps. A 250 steps history data which was 10 steps away from the current sampling instant was adopted to generate historical

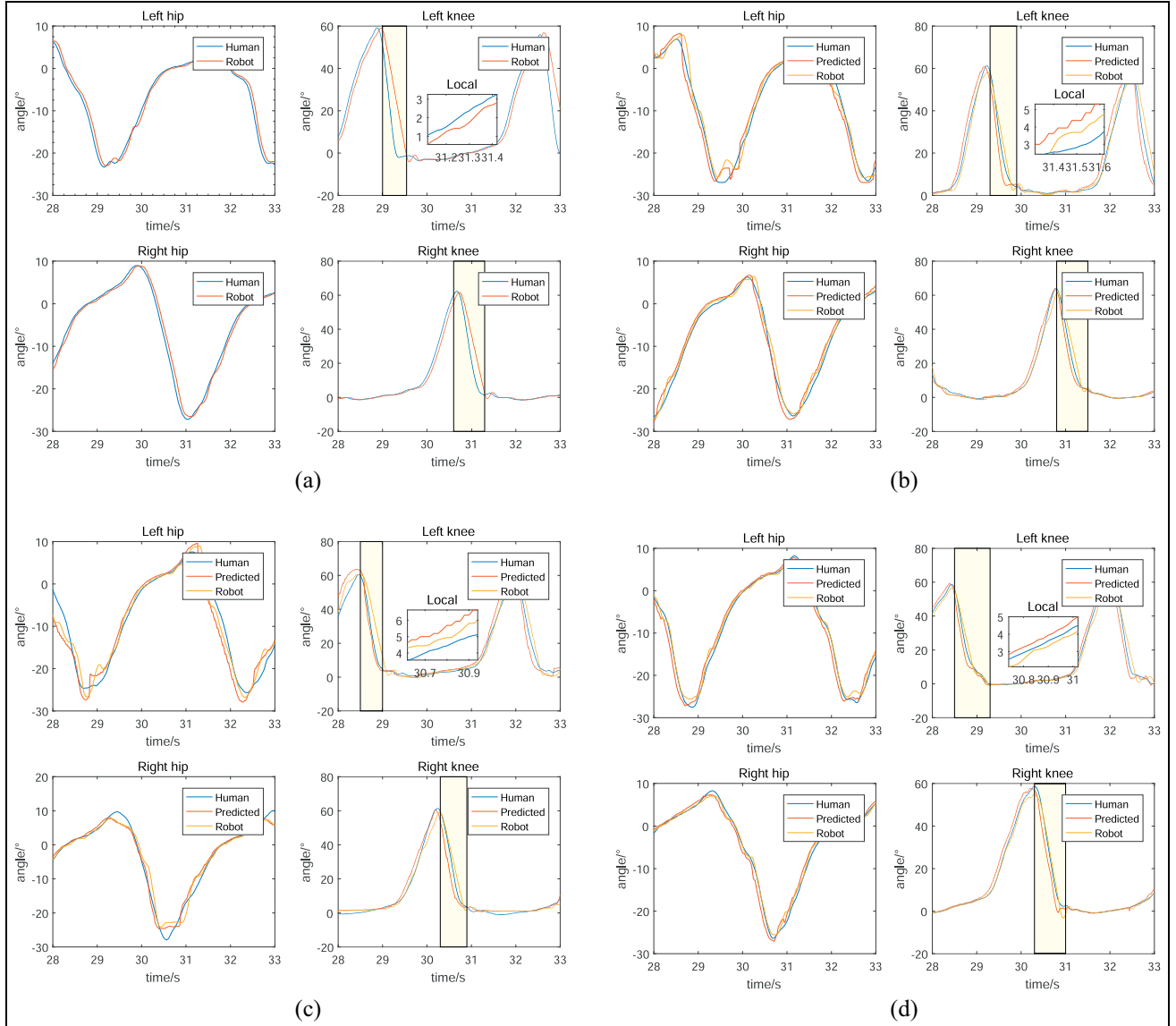


**Figure 11.** Typical cycle of walking during stable stages by different methods: (a) baseline, (b) DPSR method, (c) echo method, and (d) fused method.

embeddings. The delay of the exoskeletal robots' joints was hard to identify visually comparing with the whole time range, so in the following content typical segments were displayed rather than the whole series of data.

Figure 11 shows that the echo and DPSR methods could fill the time lag between the exoskeletal robot and its operator, but the predicted trajectories were not as accurate as the human original motion. This was especially evident in the highlighted segments of Figure 11. Although phase lead could always be observed while the echo and DPSR method applied, phase lead was not the intention of the system application. The fused method predicted trajectories were smoother and more accurate and the compensation provided very close tracking of the original human motion.

According to Table 1, the DPSR and echo methods did not present advantages over the baseline data. On the contrary, the echo method performed worse. The reasons were as follows:

1. The prediction error of the baseline experiment came only from the gap of 40–60 ms and the profile was exact. This resulted a very high PR value for the baseline experiment.
2. The predicted trajectories lacked accuracy, which counteracted with the delay compensation effect.
3. Little jumps appeared in the DPSR and echo method predicted trajectories, which brought down the TR values.

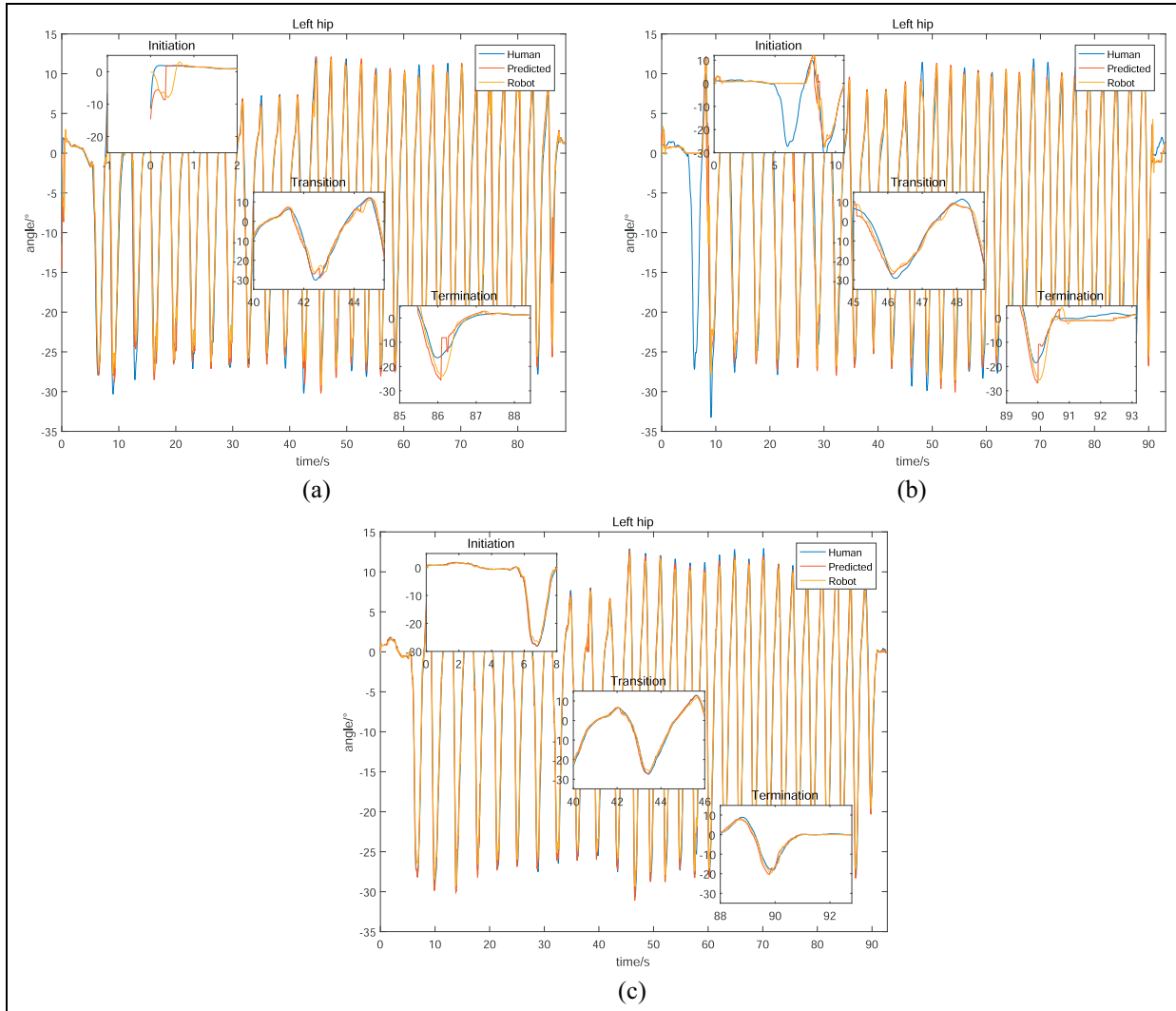


**Figure 12.** Typical errors predicted during initiation, transition, and termination by different methods: (a) DPSR prediction method, (b) echo prediction method, and (c) fused prediction method.

Intuitively, TRs would be assumed hard to improve; the prediction ability became the key limit of the OCR elevation. But this was not true in reality. The trajectories' smoothness had significant effect on the value of TRs. This was because the motor controller displayed much higher performance when the tracking trajectories were smoother. Therefore, the PRs and TRs were not independent and the TRs actually relied on the predicted trajectories. Also, smoothness was the inherent characteristic of human motion; if the predicted trajectories had little jumps over the current positions, the jumps should be corrected by the algorithm. The correction was an important part of the fused method.

The fused method with jump correction outperformed the other methods evidently. The TRs improvement with the PRs elevation in Table 1 provided strong support for the observation of the importance of

smoothness, which could also be inferred by the local view of Figure 11 visually.

Besides, the performance during initiation, transition, and termination demonstrated the characteristics of different methods. The DPSR method was history dependent, which presented sharp oscillation locally at the beginning of the initiation process with no history data, the termination process with sudden ending, and the transition process, as shown in Figure 12(a). The echo method needed the joints' data of the other side, which led to erroneous data with a length of around a half joint motion cycle during the initiation process, as shown in Figure 12(b). Figure 12(c) demonstrates that the fused method performed with excellence continuously across the whole time span.

To unveil the tracking abilities during normal conditions, the initiation and termination stages were excluded

**Table 2.** Performance of different methods including and excluding initialization and termination (ex.IT).

	Left hip			Left knee			Right hip			Right knee		
	PR	TR	OCR	PR	TR	OCR	PR	TR	OCR	PR	TR	OCR
Echo	0.762	0.899	0.751	0.818	0.705	0.628	0.860	0.913	0.837	0.864	0.842	0.846
Echo (ex. IT)	0.873	0.910	0.876	0.883	0.688	0.637	0.887	0.911	0.867	0.881	0.868	0.866
DPSR	0.869	0.895	0.842	0.870	0.746	0.727	0.885	0.907	0.855	0.904	0.871	0.842
DPSR (ex. IT)	0.884	0.907	0.856	0.860	0.753	0.740	0.886	0.907	0.855	0.902	0.867	0.839
Fused	0.964	0.943	0.933	0.957	0.831	0.823	0.966	0.944	0.933	0.962	0.917	0.911
Fused (ex. IT)	0.966	0.943	0.934	0.960	0.828	0.821	0.966	0.944	0.934	0.963	0.917	0.910

PR: prediction ratio; TR: tracking ratio; OCR: overall compensation ratio; DPSR: delay-coordinate phase space reconstruction.

from the original data and the metrics were calculated again. In Table 2, most PR, TR and OCR values of ‘Echo (ex. IT)’ exhibited visible raise when comparing with the corresponding values of ‘Echo’, while for the DPSR and fused methods such a phenomenon was not obvious. The DPSR method did not show any superior over the echo method when the initiation and termination conditions were excluded, while the fused method metrics hardly changed meaning higher robustness.

If the proposed methods were applied to the exoskeletal robot wearing by its operator, it could be deduced that the echo and DPSR method would perform even worse, because the human–robot interaction would introduce more sudden change, irregular and non-periodic movement. The solution might be eliminating the prediction and compensation when such motion was detected; yet obviously the best choice from the current experiment should be exploiting the fuse method which is more accurate and robust.

It is the same for all prediction methods that deterioration happens in long-term prediction and the compensation would be ineffective. The acceptable prediction errors depend on specific applications. For the current compensation requirement of 20–60 ms of the robot system, the method works fine. We had tested the method on the same robot system with different motor controllers exhibiting a delay between 20 and 400 ms, when the delay was higher than 200 ms, the tracking results showed unacceptable local errors from time to time which meant 200 ms was the limit for such a prediction method.

## Conclusion

Based on analyzing the inherent features of human walking, we proposed and implemented three prediction method to compensate the delay of an exoskeletal robot system while tracking its operator’s walking, including the DPSR method, echo prediction method and fused prediction method. The conventional DPSR method and the proposed echo prediction method had difficulties in providing better performance over the

uncompensated cases due to the short delay, insufficient prediction accuracy and trajectory smoothness. The proposed fused method exhibited significantly better performance with fewer prediction and execution errors even during the initiation, transition and termination phases. This validated the feasibility and efficacy of the fused method. Future work will be focused on the adaptation and implementation of the methods on patients with abnormal locomotion patterns.

## Acknowledgements

The authors would like to thank Zhengya Zhang, Minzhi Li, Xiaokang Xin, and Changcheng Li from Xeno Dynamics Co., Ltd for the hardware design and fabrication, Yuanqing Wu from University of Bologna for instruction and assistance in the article writing.

## Declaration of conflicting interests

The author(s) declared no potential conflicts of interest with respect to the research, authorship, and/or publication of this article.

## Funding

The author(s) disclosed receipt of the following financial support for the research, authorship, and/or publication of this article: This work is supported by the National Natural Science Foundation of China (U1630113) and the Fundamental Research Funds for the Central Universities.

## References

1. Rahman MH, Ouimet TK, Saad M, et al. Tele-operation of a robotic exoskeleton for rehabilitation and passive arm movement assistance. In: *Proceedings of the IEEE international conference on robotics and biomimetics*, Karon Beach, Thailand, 7–11 December 2011, pp.443–448. New York: IEEE.
2. Zhang S, Guo S and Pang M. Performance evaluation of a novel master-slave rehabilitation system. In: *Proceedings of the IEEE international conference on mechatronics and automation*, Takamatsu, Japan, 4–7 August 2013, pp.141–145. New York: IEEE.

3. Zhang W, Tomizuka M and Bae J. Time series prediction of knee joint movement and its application to a network-based rehabilitation system. In: *Proceedings of the IEEE American control conference*, Portland, OR, 4–6 June 2014, pp.4810–4815. New York: IEEE.
4. Zhang W, Chen X, Bae J, et al. Real-time kinematic modeling and prediction of human joint motion in a networked rehabilitation system. In: *Proceedings of the IEEE American control conference*, Chicago, IL, 1–3 July 2015, pp.5800–5805. New York: IEEE.
5. Yang C, Luo J, Pan Y, et al. Personalized variable gain control with tremor attenuation for robot teleoperation. *IEEE T Syst Man Cy: S* 2017; PP: 1–12.
6. Sheridan TB. Telerobotics. *Automatica* 1989; 25: 487–507.
7. Huang L. *Robotics locomotion control*. PhD Thesis, University of California, Berkeley, CA, 2005.
8. Li Z, He W, Yang C, et al. Teleoperation control of an exoskeleton robot using brain machine interface and visual compressive sensing. In: *Proceedings of the 12th world congress on intelligent control and automation*, Guilin, China, 12–15 June 2016, pp.1550–1555. New York: IEEE.
9. Novak D, Reberšek P, De Rossi SM, et al. Automated detection of gait initiation and termination using wearable sensors. *Med Eng Phys* 2013; 35: 1713–1720.
10. Kanjanapas K, Wang Y, Zhang W, et al. A human motion capture system based on inertial sensing and a complementary filter. In: *Proceedings of the ASME dynamic systems and control conference*, Palo Alto, CA, 21–23 October 2013, p.V003T40A004. New York: ASME.
11. Wang M, Wu X, Liu D, et al. A human motion prediction algorithm for non-binding lower extremity exoskeleton. In: *Proceedings of the IEEE international conference on information and automation*, Lijiang, China, 8–10 August 2015, pp.369–374. New York: IEEE.
12. Zhang W, Tomizuka M and Byl N. A wireless human motion monitoring system for smart rehabilitation. *J Dyn Sys Meas Control* 2016; 138: 111004.
13. Lin Y, Min H and Wei H. Inertial measurement unit-based iterative pose compensation algorithm for low-cost modular manipulator. *Adv Mech Eng* 2016; 8: 1–11.
14. Kanjanapas K. *Human mechatronics considerations of sensing and actuation systems for rehabilitation application*. PhD Thesis, University of California, Berkeley, CA, 2014.
15. Iqbal S, Zang X, Zhu Y, et al. Nonlinear time-series analysis of different human walking gaits. In: *Proceedings of the IEEE international conference on electro/information technology*, Dekalb, IL, 21–23 May 2015, pp.25–30. New York: IEEE.
16. Senda S, Takata N and Tsujita K. A study on lower limb's joint synergy in human locomotion with physical constraints on the knee. In: *Proceedings of the IEEE/SICE international symposium on system integration*, Fukuoka, Japan, 16–18 December 2012, pp.349–354. New York: IEEE.
17. Rosenblatt NJ, Latash ML, Hurt CP, et al. Challenging gait leads to stronger lower-limb kinematic synergies: the effects of walking within a more narrow pathway. *Neurosci Lett* 2015; 600: 110–114.
18. Pitkin MR. Effects of design variants in lower-limb prostheses on gait synergy. *J Prosthet Orthot* 1997; 9: 113–122.
19. Sanz-Merodio D, Cestari M, Arevalo JC, et al. Exploiting joint synergy for actuation in a lower-limb active orthosis. *Ind Robot* 2013; 40: 224–228.
20. Grimes DL, Flowers WC and Donath M. Feasibility of an active control scheme for above knee prostheses. *J Biomech Eng: T ASME* 1977; 99: 215–221.
21. Novak D and Riener R. A survey of sensor fusion methods in wearable robotics. *Robot Auton Syst* 2015; 73: 155–170.
22. Vallery H, van Asseldonk EH, Buss M, et al. Reference trajectory generation for rehabilitation robots: complementary limb motion estimation. *IEEE T Neur Sys Reh* 2009; 17: 23–30.
23. Broer H and Takens F. Reconstruction and time series analysis. In: Broer H and Takens F (eds) *Dynamical systems and chaos*. New York: Springer, 2011, pp.205–242.
24. Herrmann C. *Robotic motion compensation for applications in radiation oncology*. PhD Thesis, University of Würzburg, Würzburg, 2013.
25. Yang C, Wang X, Cheng L, et al. Neural-learning-based telerobot control with guaranteed performance. *IEEE T Cybernetics* 2017; 47: 3148–3159.
26. Yang C, Wang X, Li Z, et al. Teleoperation control based on combination of wave variable and neural networks. *IEEE T Syst Man Cy: S* 2017; 47: 2125–2136.